

Titanium isotopic anomalies, titanium mass fractionation effects, and rare earth element patterns in Allende CAIs and their relationships. A. M. Davis^{1,2,3}, J. Zhang^{1,3,*}, J. Hu^{1,3}, N. D. Greber^{1,3}, and N. Dauphas^{1,2,3}, ¹Department of the Geophysical Sciences, ²Enrico Fermi Institute, ³Chicago Center for Cosmochemistry, The University of Chicago (a-davis@uchicago.edu); *Present address: Hong Kong.

Introduction: Mass fractionation effects in Mg, Si, and Ca in CAIs have been known for several decades [1]. Non-mass-dependent anomalies in ⁵⁰Ti in CAIs and bulk meteorites have also been known for decades, but have received renewed interest in recent years with the development of multicollector inductively coupled mass spectrometry (MC-ICPMS). Although ⁵⁰Ti variations have been well known for some time, a correlated anomaly in ⁴⁶Ti in bulk meteorites has been found [2,3]. We report here both mass-dependent fractionation (MDF) and non-mass-dependent (NMD) Ti isotopic compositions of 32 Allende CAIs. We also measured rare-earth element (REE) patterns of many of the samples, since a correlation between the magnitude of Ca mass fractionation effects and volatility controlled REE patterns has been reported [4].

Methods: The CAIs are from four Allende slabs (AL8,S8; AL10,S2; AL3,S5; AL,ASU). They were drilled out using a microdrill system, with the drilling diameter of 500 μm and the drilling depth of $\sim 250 \mu\text{m}$. One or two spots were drilled for each CAI. After sample digestion, Ti was separated via a two-stage procedure using TODGA and AG1-X8 resins [5]. The full procedural blank is $\sim 10 \text{ ng}$. Ti isotopic analyses were obtained with a Thermo Neptune MC-ICPMS using sample-standard bracketing technique at high resolution [5]. The bracketing standard is natural rutile from Kragerøe, Norway purified by column chemistry. The measured Ti isotopic compositions including both Ti MDF and NMD effects are expressed in δ' notation. Ti NMD effects are reported in ϵ notation after normalization to $^{49}\text{Ti}/^{47}\text{Ti} = 0.749766$ [5] and correcting for MDF using an exponential law.

In order to test the precision of Ti mass fractionation measurements by sample-standard bracketing, we measured Ti isotopes in seven sample solutions by double spiking using a newly developed method [6]. For these measurements, an aliquot of the solution obtained after dissolution of the CAI was double-spiked and chemically purified. There is a good correlation between double-spiked and sample-standard bracketing measurements (Fig. 1), indicating that the latter have uncertainties of about 0.5‰, much smaller than the overall range of 7‰.

The solutions from the first ten samples were consumed in the initial Ti isotopic analyses, but the solutions from the remaining 22 samples were used to measure rare earth element patterns by MC-ICPMS [7]. Since the microdrilled samples were not weighed (in order minimize sample loss), we assumed that all analyzed CAIs contained 1.28 wt% Ti, the average Ti content of CAIs. This

leads to uncertainties in overall REE concentrations of at least a factor of two, but does not affect REE patterns.

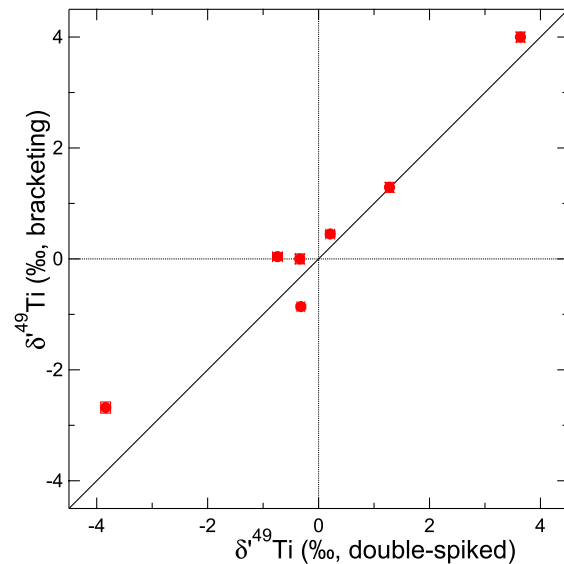


Fig. 1. Data measured by sample-standard bracketing are well correlated with double spiked data.

Each CAI was x-ray mapped and imaged in backscattered electrons in the slab surface. We further examined the slab after microdrilling to identify minerals by x-ray microanalysis. This clearly did not provide a thorough petrographic description of each CAI, but did allow classification into coarse- and fine-grained types and subdivision of coarse-grained CAIs into Types A and B.

Results and discussion: CAIs have $\delta^{xx}\text{Ti}/^{47}\text{Ti}$ values following or paralleling the MDF lines determined by evaporating perovskite [8], depending on whether there are NMD effects. The range in MDF effects is quite large, extending from $\delta^{49}\text{Ti}/^{47}\text{Ti}$ of -3 to $+4$ ‰. This is in contrast to Ca, where MDFs range from near normal to isotopically light compositions; isotopically heavy Ca only occurs in FUN CAIs [1]. After internal normalization to $^{49}\text{Ti}/^{47}\text{Ti}$, we found that the Ti anomalies of $\epsilon^{50}\text{Ti}$ and $\epsilon^{46}\text{Ti}$ in CAIs are highly correlated, but variable in magnitude, in contrast to the constant magnitude anomalies reported two Allende and two Efremovka CAIs [2]. The linear correlation between $\epsilon^{50}\text{Ti}$ and $\epsilon^{46}\text{Ti}$ extends the same correlation seen among bulk solar system objects. This observation provides constraints on the dynamic mixing of the solar disk.

The CAIs have a variety of REE patterns, but basically can be subdivided into relatively unfractionated Group I and volatility fractionated Group II patterns (Fig. 2). There are some interesting features in the light REE

that are controlled by volatility also, but these will not be explored in detail here.

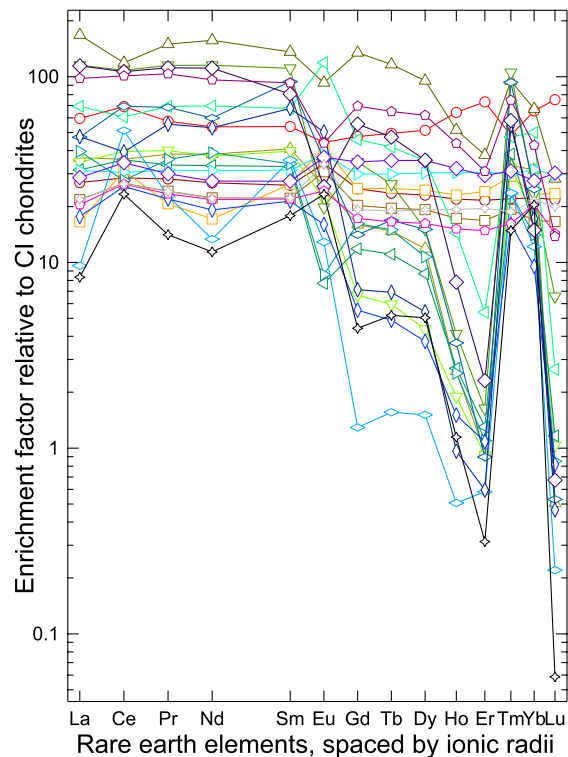


Fig. 2. REE patterns in 22 of the 32 CAIs analyzed for Ti isotopes, normalized to CI chondrite abundances [7].

A correlation has been reported between REE patterns and Ca MDF isotopic effects, with CAIs having Group II REE patterns having more isotopically light Ca. Despite Ti showing a somewhat wider range of MDF effects, no such correlation was found between REE patterns and (Fig. 3). Here we plot $\delta^{49}\text{Ti}/^{47}\text{Ti}$ vs. CI normalized Lu/La ratios, as Lu is strongly depleted relative to La in Group II CAIs and undepleted in Group I. There does seem to be a wider range of $\delta^{49}\text{Ti}/^{47}\text{Ti}$ values among Group II CAIs, suggesting kinetically controlled volatility fractionation of Ti during REE fractionation. This makes sense as high temperatures are required for both kinds of fractionation, but it is not clear why both isotopically heavy and light Ti is found in Group II CAIs. Formation of Group II REE patterns requires removal of an ultrarefractory dust followed by condensation of the remaining gas [9,10].

There is also no correlation between $\epsilon^{50}\text{Ti}$ and REE patterns (Fig. 4). This is perhaps less surprising than the lack of correlation between REE patterns and Ti MDF effects. There is a significant range in the magnitude of $\epsilon^{50}\text{Ti}$ among CAIs, in contrast to the relatively constant values found in four Allende and Efremovka CAIs [2].

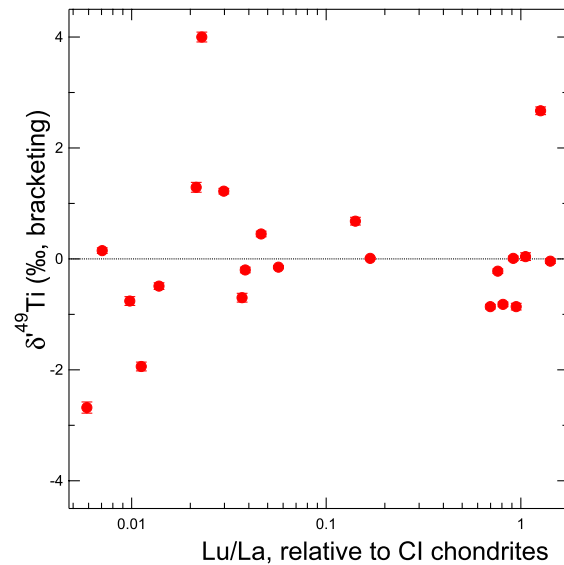


Fig. 3. There is no correlation between Ti MDF effects and REE patterns, although Group II CAIs have a wider range of MDF effects.

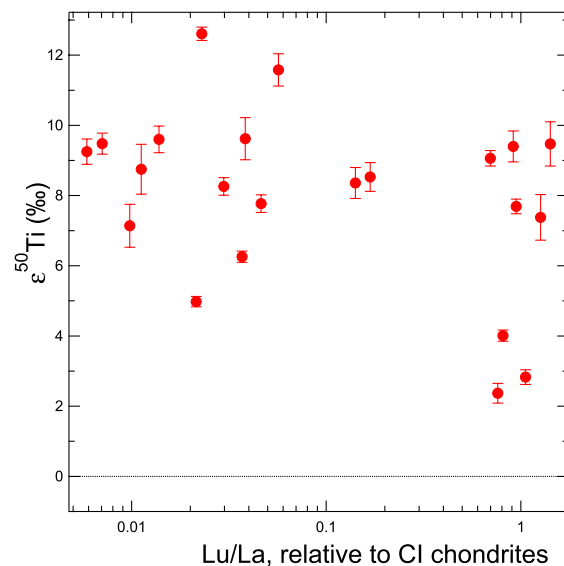


Fig. 4. There is no correlation between ^{50}Ti anomalies and REE patterns.

References: [1] Clayton R. N. et al. (1988) *Phil. Trans. R. Soc. Lond.*, A325, 483. [2] Trinquier A. et al. (2009) *Science*, 324, 374. [3] Zhang J. et al. (2012) *Nature Geosci.*, 5, 251. [4] Huang S. et al. (2011) *Geochim. Cosmochim. Acta*, 77, 252. [5] Zhang J. et al. (2011) *J. Anal. At. Spectrom.*, 26, 2197. [6] Millet M.-A. (2014) *J. Anal. At. Spectrom.*, 29, 1444. [7] Pourmand A. et al. (2012) *Chem. Geol.*, 291, 38. [8] Zhang J. et al. (2014) *Geochim. Cosmochim. Acta*, 140, 365. [9] Boynton W. V. (1975) *Geochim. Cosmochim. Acta*, 39, 569. [10] Davis A. M. & Grossman L. (1979) *Geochim. Cosmochim. Acta*, 43, 1611.